Title
Transport and burial rates of10Be and231Pa in the Pacific Ocean during the Holocene period

Journal
Earth and Planetary Science Letters, 113(1-2)

ISSN
0012-821X

Authors
Lao, Yong
Anderson, Robert F
Broecker, Wallace S
et al.

Publication Date
1992-09-01

DOI
10.1016/0012-821x(92)90218-k

Earth and Planetary Science Letters, 113 (1992) 173–189
Elsevier Science Publishers B.V., Amsterdam

[CL]

Transport and burial rates of ^{10}Be and ^{231}Pa in the Pacific Ocean during the Holocene period

Yong Lao [a], Robert F. Anderson [a], Wallace S. Broecker [a], Susan E. Trumbore [b]*, Hansjakob J. Hofmann [b] and Willy Wolfli [b]

[a] *Lamont-Doherty Geological Observatory of Columbia University, Palisades, NY 10964, USA*
[b] *Institut fur Mittelenergiephysik, ETH-Honggerberg, CH-8095, Zurich, Switzerland*

Received January 15, 1992; revision accepted June 19, 1992

ABSTRACT

An ocean-wide study of the rates of removal of ^{10}Be and ^{231}Pa in the Pacific Ocean has identified intensified scavenging of the ^{10}Be and ^{231}Pa in several ocean margin areas, including the Northeastern and Northwestern Pacific, the Bering Sea, the Eastern Equatorial Pacific and the South Pacific Ocean. Scavenging rates of ^{10}Be and ^{231}Pa are clearly correlated to particle flux Principal component analysis further suggests that scavenging of ^{10}Be and ^{231}Pa may be related to opal productivity in surface waters A simple box model was constructed to partition the deposition of ^{230}Th, ^{231}Pa and ^{10}Be between open ocean and ocean margin sediments. Model parameters were constrained using measured values of ^{230}Th and ^{231}Pa, which have a common source, and then applied to ^{10}Be. An average Holocene ^{10}Be deposition rate for the entire Pacific Ocean is estimated to be $\sim 1.5 \times 10^6$ atoms/cm^2 yr^{-1}, with $\sim 70\%$ of the total ^{10}Be supplied to the Pacific being deposited in margin sediments underlying only 10% of the ocean. The short residence times of ^{10}Be in ocean margin regions (from < 100 to ~ 200 yr) compared to the long ^{10}Be residence time in the central open Pacific Ocean (~ 1000 yr) reflects the intensified scavenging of ^{10}Be in ocean margin waters. The results of this study suggest that the Pacific Ocean acts as a relatively closed basin with respect to the transport and burial of ^{10}Be; therefore, the average ^{10}Be deposition rate in the Pacific Ocean can be used as an estimate of the global average production rate of ^{10}Be in the atmosphere during the Holocene period.

1. Introduction

^{10}Be ($t_{1/2} = 1.5 \times 10^6$ yr) is produced in the upper atmosphere by spallation of oxygen and nitrogen atoms by galactic cosmic rays [1]. Many applications of ^{10}Be as a geochemical tracer require the atmospheric production rate of ^{10}Be to be accurately known (see [2] for a review). One of the ways of estimating the global average ^{10}Be production rate involves measurement of ^{10}Be in deep-sea sediments. Initial estimates of the deposition rate of ^{10}Be from deep-sea cores in the open Pacific Ocean were in close agreement with theoretical calculations, ranging mostly from about 0.4 to 1.2×10^6 atoms/cm^2 yr^{-1} [3–5]. Studies of deep-sea cores in the open Atlantic Ocean [6,7] yielded a rate of $\sim 0.6 \times 10^6$ atoms/cm^2 yr^{-1} which is on the lower side of the theoretical calculations. As more and more results emerged, tremendous differences among ^{10}Be deposition rates at different locations in the oceans became apparent. A deposition rate of 8.3×10^6 atoms/cm^2 yr^{-1} was detected in sediments accumulated off Africa [8]; about the same rate of 11×10^6 atoms/cm^2 yr^{-1} is derived from ^{10}Be results in sediments off the coast of California [9] and in Northwest Pacific margin sediments [10]. The highest ^{10}Be deposition rate ($\sim 60 \times 10^6$ atoms/cm^2 yr^{-1}) was observed in the Zaire deep-sea fan in the Angola Basin [11], while an extremely low deposition rate ($\sim 0.02 \times 10^6$

Correspondence to: Yong Lao, Lamont-Doherty Geological Observatory of Columbia University, Palisades, NY 10964, USA.
* Present address: Department of Geosciences, University of California at Irvine, CA 92717, USA.

TABLE 1

Locations, sediment types and sedimentation rates of the cores in the Pacific Ocean.

Core	Latitude	Longitude	Depth (m)	Map site	Sediment type	Sedimentation rate (cm/kyr) [1]
RC14-121	54°51'N	170°41'W	2532	1	Hemipelagic, rich in diatoms	20
V20-122	46°34'N	161°41'E	5563	2	Hemipelagic	4.5
RC14-105	39°41'N	157°33'E	5630	3	Hemipelagic	6.0
V21-146	37°41'N	163°02'E	3968	4	Hemipelagic	3.8
V32-126	35°19'N	174°54'E	3870	5	Pelagic, red clay	2.3
V32-128	36°27'N	177°09'E	3623	6	Pelagic, red clay	1.7
MANOP Site R	38°N	158°W	5800	7	Pelagic, red clay	0.2
V20-88TW	40°11'N	151°39'W	5081	8	Pelagic, red clay	0.2
V20-85TW	44°54'N	143°37'W	3817	9	Pelagic, calcareous ooze	0.3
W8709A-1BC	41°33'N	131°57'W	3680	10	Pelagic, red clay	1.3
W8709A-8TC	42°16'N	127°41'W	3111	11	Hemipelagic	10
W8709A-13(T)PC	42°07'N	125°45'W	2712	12	Hemipelagic	20
Point Sur BC116	36°06'N	122°36'W	3340	13	Hemipelagic	5.4
Point Sur BC133	36°12'N	122°16'W	1210	14	Hemipelagic, sandy	15
Point Sur BC150	36°11'N	122°22'W	1585	15	Hemipelagic	8
Point Sur BC151	35°38'N	121°37'W	787	16	Hemipelagic	9.4
San Clemente QP2	32°35'N	118°10'W	1945	17	Hemipelagic	15
MANOP Site S	11°03'N	140°05'W	4904	18	Pelagic, siliceous ooze	< 0.1
V21-59	20°55'N	158°06'W	2992	19	Pelagic, calcareous ooze	0.8
V35-05	07°12'N	112°05'E	1953	20	Hemipelagic	15
V28-238	01°01'N	160°29'E	3120	21	Pelagic, calcareous ooze	1.7
RC11-210	01°49'N	140°03'W	4420	22	Pelagic, calcareous ooze	1.2
MANOP Site C	01°02'N	138°56'W	4423	23	Pelagic, calcareous ooze	1.7
V19-28	02°22'S	84°39'W	2720	24	Hemipelagic	5.0
V19-29	03°35'S	83°56'W	3157	25	Hemipelagic	10
TT154-10	10°17'S	111°20'W	3225	26	Pelagic, rich in metal oxides	2.0
V19-55	17°00'S	114°11'W	3177	27	Pelagic, rich in metal oxides	1.2
V18-299	16°07'S	149°40'W	4284	28	Pelagic, calcareous ooze	0.6
RC8-81TW	47°57'S	159°03'W	5130	29	Pelagic, red clay	0.2
E17-9(PC,TC)	63°05'S	135°07'W	4848	30	Pelagic, rich in opal	3.6
E15-6TC	59°58'S	101°19'W	4517	31	Pelagic, rich in opal	3.7
RC15-61	40°37'S	77°12'W	3771	32	Hemipelagic	3.8

[1] The sedimentation rates for most of the cores were from literature (see detailed list of references in [26]). Those for the following cores were based on this work: for the Point Sur cores (BC116, 133, 150, and 151) they were estimated to be the same as that of several cores in a nearby area dated by the ^{14}C method (C. Reimers, unpublished data); San Clemente QP2 was dated by ^{14}C counting of total carbon extracted from the core; for V18-299, it was obtained by plotting unsupported ^{230}Th and ^{231}Pa against depth of the core; for RC8-81, it was uncertain and tentatively assigned as 0.2 cm/kyr (close to those of red clay cores in the North Pacific) based on the great water depth and the red clay content of the core.

atoms/cm^2 yr^{-1}) was reported in the Arctic Ocean [12]. It is obvious that the deposition rate of ^{10}Be at a single site, or even an average of a few sites in the ocean, can not provide a reliable estimate of the global average production rate of ^{10}Be. A more comprehensive understanding of the marine geochemistry of ^{10}Be is required before its deposition rate in the ocean may be used as an estimate of its global average production rate.

Intensified scavenging in ocean margin areas (i.e., boundary scavenging) was shown to greatly influence the removal of particle-reactive chemical substances such as ^{210}Pb [13–16], Pu isotopes [17] and ^{231}Pa [18–22] in the ocean. The results of previous studies [9,10] and our work [23–25] have shown that ^{10}Be is also preferentially removed from the oceans in some margin areas. In order to evaluate the source of ^{10}Be, and to understand its transport within the oceans, we need to conduct an ocean-wide study: (1) to estimate the extent to which ^{10}Be deposition is enhanced in different ocean margin regions; and (2) to examine what factors influence the scavenging of ^{10}Be from seawater to sediments. After the behavior of ^{10}Be in various marine environments is well understood, we will be in a better position to use ^{10}Be as a geochemical and geophysical tracer. This paper presents an overview of Pacific-wide boundary scavenging of ^{10}Be and ^{231}Pa during the Holocene period (i.e., the last 10,000 yr).

2. Core selection and results

Sediments from deep-sea cores in the Pacific were analyzed for U, ^{230}Th, ^{231}Pa and ^{10}Be nuclides and major and trace elements [26]. ^{230}Th and ^{231}Pa are radioactive nuclides ($t_{1/2}$ = 75,200 and 32,500 yr, respectively) which decay with time. Therefore, it is necessary to make decay corrections on cores that have age information to obtain the initial unsupported concentrations for ^{230}Th and ^{231}Pa (i.e., the fractions of ^{230}Th and ^{231}Pa that are only produced by decay of dissolved ^{234}U and ^{235}U, respectively, in the water column). Since the half-life of ^{10}Be is relatively long (1.5×10^6 yr) compared to that of ^{230}Th and ^{231}Pa, it is unnecessary to make decay corrections for ^{10}Be for the purpose of studying deep-sea sediments accumulated during the last 10,000 years.

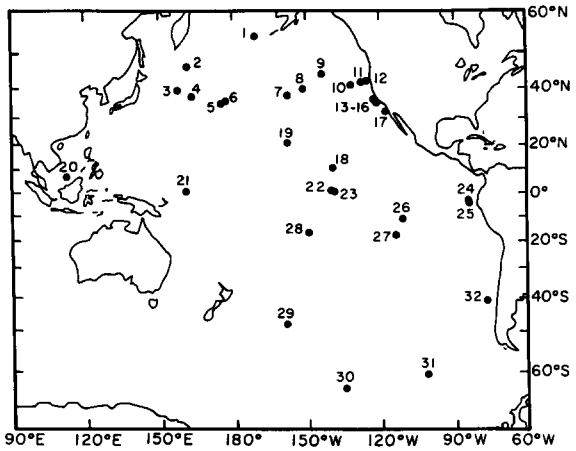

Fig. 1. Map of core sites in this study. Numbers = the map sites listed in Table 1.

Cores that had stratigraphic controls such as ^{18}O, ^{14}C and ^{13}C isotope results were preferred. In some areas where stratigraphic information was unavailable but otherwise useful cores could be obtained, the sedimentation rates of the cores were estimated in two ways. One was to measure downcore unsupported ^{230}Th and ^{231}Pa concentrations and then construct an average sedimentation rate for the core of interest. The second was by comparing the core of interest to nearby cores for which stratigraphic information was available. The principal criteria for core selection were that the chronologies of the cores should be of good quality, representative of a variety of marine environments, and readily accessible [26]. Thirty-two cores that were believed to best serve our purposes were selected (Table 1, Fig. 1).

Five cores (V20-122, RC14-105, V21-146, V32-126 and V32-128) were chosen from the Northwest Pacific where work has been carried out to study eolian dust input from Asia [27,28]. A vast area in the central North Pacific gyre region is covered by red clay sediment which originates from eolian dust, and sedimentation rates in such an area are usually < 5 mm/ky [29,30]. It is important to know what role the area of very low sedimentation plays in ^{231}Pa and ^{10}Be deposition. Four cores (V20-85, V20-88, MANOP Site R and Site S) that have sedimentation rates of ~ 2 mm/ky were thus included. Intensified scavenging of ^{231}Pa (relative to ^{230}Th) was found in the Northeastern Pacific [20] where we selected eight

TABLE 2

Concentrations of U, Th, Pa, $^{230}Th_{xs,o}$, $^{231}Pa_{xs,o}$ (all in dpm/g), ^{10}Be (10^9 atoms/g), and ratios of $(Pa/Th)_{xs,o}$ and $Be/_{xs}Th_o$ (10^9 atoms/dpm) [1]

Core (cm)	Age (ka)	^{238}U	^{232}Th	^{230}Th	^{231}Pa	^{10}Be	$^{230}Th_{xs,o}$	$^{231}Pa_{xs,o}$	$(Pa/Th)_{xs,o}$	$Be/_{xs}Th_o$
RC14-121										
25–27	1.2	1.67±0.04	0.43 ±0.02	1.57±0.05	0.20±0.01	1.36±0.03	1.22±0.11	0.19±0.01	0.154±0.016	1.116±0.105
45–47	2.1	2.38±0.07	0.44 ±0.02	1.74±0.04	0.23±0.01	1.34±0.03	1.38±0.13	0.22±0.01	0.158±0.017	0.974±0.094
V20-122										
8–10	2.0	0.71±0.02	0.85 ±0.03	16.0 ±0.32	2.21±0.09	5.25±0.10	15.6 ±0.37	2.27±0.10	0.145±0.007	0.336±0.010
26–28	6.0	0.83±0.02	0.97 ±0.04	10.9 ±0.26	1.39±0.06	3.82±0.07	10.7 ±0.34	1.54±0.07	0.144±0.007	0.357±0.014
RC14-105										
10–12	1.8	1.09±0.04	1.86 ±0.07	30.8 ±0.95	2.66±0.10	6.00±0.10	29.8 ±1.00	2.69±0.10	0.090±0.005	0.201±0.008
32–33	5.3	0.87±0.03	1.11 ±0.04	9.3 ±0.22	0.85±0.04	3.39±0.08	8.88±0.33	0.91±0.04	0.102±0.006	0.382±0.017
V21-146										
10–11	2.8	0.69±0.02	1.27 ±0.05	14.9 ±0.32	1 30±0.06	3.75±0.05	14.3 ±0.42	1.33±0.06	0.093±0.005	0.262±0.007
24–25	6.4	0.71±0.02	1.26 ±0.05	9.57±0.21	0.88±0.03	2.66±0.06	9.10±0.35	0.96±0 04	0.105±0.005	0.293±0.010
V32-126										
7–8	3.3	0.62±0.02	1.24 ±0.05	20.7 ±0.45	1.25±0.05	2.19±0.03	20.3 ±0.46	1.29±0.05	0.064±0.003	0.108±0.003
16–17	7.3	0.71±0.02	1.49 ±0.06	12.6 ±0.31	0.83±0.04	3.49±0.06	12.3 ±0.34	0.91±0.05	0.074±0.005	0.284±0.012
V32-128										
8–10	5.2	0 43±0.02	0.92 ±0.03	15.5 ±0.38	0.90±0.06	2.90±0.07	15.5 ±0.45	0.97±0.07	0.062±0.005	0.187±0.007
12–13	7.3	0.47±0.02	0.83 ±0.03	17.8 ±0.35	1.18±0.07	2.87±0.05	18.4 ±0.41	1.35±0.08	0.073±0.005	0.156±0.004
MANOP R										
0–5(1)[3]	15?[2]	1.83±0.04	3.77 ±0.17	75.5 ±1.64	2.74±0.12	5.77±0.14	83.5 ±2.10	3.60±0.16	0.043±0.002	0.069±0.002
0–5(2)[3]	15?	1.72±0.04	3.58 ±0.16	72.4 ±1.51	2.37±0.11	5.50±0.10	80.0 ±1.94	3 10±0.15	0.039±0.002	0.069±0.002
V20-88										
Top	15?	1.50±0.05	3.61 ±0.18	51.5 ±1.33	1.90±0.07	8.58±0.15	50.1 ±1.74	2.46±0.11	0.044±0.002	0.153±0.006
V20-85										
0–1	15?	1.18±0.04	2.58 ±0.11	24.2 ±0.51	0.90±0.04	6.26±0.09	25.6 ±0.59	1.12±0.06	0.044±0.002	0.244±0.009
W8709A-1										
1–3	5.0	1.43±0.04	2.68 ±0.09	45.7 ±1.19	3.43±0.10	7.32±0.10	45.7 ±1.37	3.71±0.11	0.081±0.003	0.160±0.005
7–9	5.6	1.37±0.03	2.69 ±0.09	43.6 ±1.17	3.54±0.09	7.17±0.13	43.7 ±1.38	3 88±0.10	0.089±0.003	0.164±0 006
W8709A-8										
9–10	1.0	1 50±0.04	1.53 ±0.04	8.30±0.20	1.32±0.04	3.57±0 07	7.13±0.37	1.29±0.04	0.180±0.011	0.501±0.028
44–45	4.1	2.26±0 05	1.62 ±0.06	7.96±0.21	1.25±0.04	3.58±0.06	6.90±0.41	1.30±0.04	0.188±0 013	0.518±0.032
W8709A-13										
4–5	4.7	2.46±0.04	1.35 ±0.05	3.00±0.09	0.44±0.02	1.99±0.04	1.93±0.30	0.42±0.02	0.217±0.036	1.033±0.163
18–20	5.4	3.25±0.06	1.37 ±0.07	2.90±0.08	0.37±0.01	1.82±0.03	1.77±0.32	0.35±0.02	0.196±0.037	1 037±0.183
PS BC166										
0–1	1.0	1.99±0.06	2.17 ±0.05	6.09±0.12	0.78±0.03	3.00±0.04	4.48±0.14	0.72±0.04	0.163±0.019	0.523±0.056
9–11	1.8	4.31±0.09	2.28 ±0.07	6.09±0.15	0.87±0.03	2 69±0.05	4.31±0.17	0.81±0.04	0.189±0.024	0.624±0.074
PS BC133										
0–1	2.0	0.59±0.02	0.89 ±0.03	1.99±0.05	1.24±0.05	18.9±0.85	1.31±0.06	1.26±0.05	0.966±0.058	14.45 ±2.20
10–12	2.0	0.78±0.02	1.08 ±0.03	1.99±0.05	0.87±0.03	16 1±0.43	1.15±0.06	0.87±0.03	0.754±0.046	14.01 ±2.80
PS BC150										
0–1	1.0	1.98±0.08	2.20 ±0.07	3.73±0.10	0.45±0.02	1.66±0.03	1.99±0.47	0.38±0.02	0.190±0.047	0.834±0.197
8–10	5.0	2.87±0.11	2.31 ±0.08	3 74±0.12	0.49±0.02	1.65±0.02	1.93±0.52	0.41±0.02	0.217±0.065	0.866±0.231

PS BC151										
0–1[4]	1.0	2 48 ± 0.05	2.20 ± 0.06	2.92 ± 0.07	0.26 ± 0.01	0.83 ± 0.03	1 16 ± 0.46	0.18 ± 0.02	0.157 ± 0.015	0.711 ± 0.280
8–10[4]	1 0	3.29 ± 0.06	2.55 ± 0.06	3.28 ± 0.07	0.28 ± 0.01	0.71 ± 0.06	1.24 ± 0.40	0.19 ± 0.02	0.153 ± 0.015	0.573 ± 0.248
SCB QP2										
0–10	1.0	2.27 ± 0.07	1.96 ± 0.08	7.79 ± 0.26	1.29 ± 0.04	2.24 ± 0.05	6 27 ± 0.27	1.24 ± 0.04	0.198 ± 0.011	0.358 ± 0.030
10–15	1.0	3.05 ± 0.08	1.69 ± 0.08	6.65 ± 0.17	1.03 ± 0.03	2.64 ± 0.04	5.33 ± 0.17	0.99 ± 0.03	0.185 ± 0.009	0.496 ± 0.038
MANOP S										
1.5–2.1	15?	1.26 ± 0.03	3.55 ± 0.121	80.7 ± 2.9	3.88 ± 0.15	5.67 ± 0.08	204.5 ± 3.4	5 19 ± 0.21	0.025 ± 0.001	0.028 ± 0.001
0–2	15?	1.27 ± 0.03	3.66 ± 0.231	78.9 ± 4.7	4.40 ± 0.18	n.d.	202.2 ± 5.4	5.90 ± 0.25	0.029 ± 0.001	n.d.
V21-59										
5–6	7.1	0.59 ± 0.02	0.33 ± 0.02	17.5 ± 0.38	1.29 ± 0.05	1.75 ± 0.04	18.4 ± 0 41	1.48 ± 0.06	0 081 ± 0.004	0.095 ± 0.003
7–8	9.6	0.64 ± 0 02	0.32 ± 0.02	15.9 ± 0.25	1.14 ± 0.05	1.79 ± 0.04	17.0 ± 0 55	1.38 ± 0.06	0 082 ± 0.004	0.105 ± 0.004
V35-05										
70–75	7.0	2.09 ± 0 08	3.05 ± 0.09	3.16 ± 0.09	n.d	1.17 ± 0.02	0 96 ± 0.04	n.d.	n.d.	1.466 ± 1.236
V28-238										
0–8	4 8	0.20 ± 0.01	0.137 ± 0.007	8.98 ± 0.14	0.56 ± 0.03	1.15 ± 0.05	9.27 ± 0.15	0.62 ± 0.03	0.067 ± 0.003	0.124 ± 0.005
14–16	8.5	0.18 ± 0.01	0.142 ± 0.008	8 20 ± 0.13	0.45 ± 0.02	1.24 ± 0 05	8.74 ± 0.14	0.54 ± 0.02	0.062 ± 0.003	0.142 ± 0.006
RC11-210										
5–7(1)[3]	6.0	0.17 ± 0.01	0.108 ± 0.005	23.6 ± 0.29	1.60 ± 0.06	n.d.	24.8 ± 0.30	1.81 ± 0.07	0.073 ± 0.003	n.d.
5–7(2)[3]	6.0	0.17 ± 0.01	0.090 ± 0.005	22.6 ± 0.31	1.45 ± 0.04	2.95 ± 0.10	23.9 ± 0.33	1.64 ± 0.07	0.069 ± 0.002	0.123 ± 0.004
MANOP C										
1.5–2.1[4]	6.0	0.20 ± 0.006	0.148 ± 0.020	25.7 ± 0.41	1.51 ± 0 05	0.96 ± 0.06	26.9 ± 0.14	1.71 ± 0.06	0.064 ± 0.002	0.036 ± 0.002
3.6–4.2[4]	6.0	0.19 ± 0.006	0.113 ± 0.021	23.3 ± 0.38	1.56 ± 0.06	1.51 ± 0.14	24 5 ± 0.41	1.77 ± 0.07	0.072 ± 0.003	0.062 ± 0.006
V19-28										
17–19	5.3	1.48 ± 0.06	0.192 ± 0.010	5.18 ± 0.12	0.94 ± 0.03	3.15 ± 0.09	5.21 ± 0.14	1.04 ± 0.04	0.200 ± 0 009	0.604 ± 0.024
V19-29										
17–19	1.8	1.56 ± 0.06	0.511 ± 0.023	6 38 ± 0.15	1.08 ± 0.05	5 32 ± 0.13	6.05 ± 0.20	1.10 ± 0.05	0.183 ± 0.010	0.879 ± 0.036
45–47	4.5	5.39 ± 0.19	0.414 ± 0.021	5.39 ± 0.13	0.82 ± 0.04	4.16 ± 0.10	5.03 ± 0.28	0.86 ± 0.05	0.171 ± 0.010	0.827 ± 0.050
TT154-10										
1.2–2.4	5.9	0.47 ± 0.02	0.020 ± 0.003	13.78 ± 0.20	1.93 ± 0.07	2.63 ± 0.09	14 5 ± 0.21	2.19 ± 0.08	0.151 ± 0.006	0.181 ± 0.007
4.2–6.0	6.8	0.48 ± 0 02	0.015 ± 0.004	13.42 ± 0.22	2.01 ± 0.06	2.26 ± 0.06	14.2 ± 0.24	2.32 ± 0.06	0.163 ± 0.005	0.159 ± 0.005
V19-55										
0–2	5 1	1 32 ± 0.05	0.022 ± 0.006	20.42 ± 0.28	2.84 ± 0.10	4.13 ± 0.12	21.3 ± 0.30	3.16 ± 0.11	0.148 ± 0.005	0.194 ± 0.006
8–10	7 7	1.56 ± 0.06	0.033 ± 0.004	19.32 ± 0.30	2.41 ± 0.08	3.96 ± 0.11	20.6 ± 0.32	2.83 ± 0.10	0.137 ± 0.005	0.192 ± 0.006
V18-299										
0–5	6.0	0.98 ± 0.04	1.165 ± 0.035	72.10 ± 1.02	2.93 ± 0.15	9.52 ± 0.32	75.2 ± 1 10	3.29 ± 0.17	0.044 ± 0.002	0.127 ± 0.004
RC8-81										
3–4	15?	1.21 ± 0.04	2.34 ± 0.11	38.8 ± 0.71	2.35 ± 0.07	4.29 ± 0.06	42.5 ± 0.98	3.13 ± 0.10	0.073 ± 0.003	0.101 ± 0.003
E15-6										
4–7(1)[5]	1.5?	0.63 ± 0 01	0.84 ± 0.04	20.0 ± 0.50	1.87 ± 0.10	5.54 ± 0 09	19.6 ± 0.54	1.90 ± 0.10	0.097 ± 0.006	0.282 ± 0.009
4–7(2)[5]	1.5?	0.59 ± 0 01	0.78 ± 0.03	22.6 ± 0.57	2.21 ± 0.07	8.10 ± 0 10	22.3 ± 0.60	2.25 ± 0.07	0.101 ± 0.004	0.364 ± 0.010
E17-9										
7–10(1)[5]	2 4	0.59 ± 0.02	0.54 ± 0.02	17.9 ± 0.40	2.54 ± 0.07	5.31 ± 0.12	17.9 ± 0.41	2.65 ± 0.07	0.148 ± 0.005	0.296 ± 0.010
7–10(2)[5]	2 4	0.54 ± 0.02	0.49 ± 0.02	17.3 ± 0.39	2.53 ± 0.09	5.04 ± 0.24	17.2 ± 0.40	2.64 ± 0.10	0 153 ± 0.007	0.292 ± 0.016
RC15-61										
6–9	2 0	0.74 ± 0.03	1.16 ± 0.03	12.3 ± 0.23	0.88 ± 0.04	2.92 ± 0.07	11.7 ± 0.34	0.87 ± 0.04	0.075 ± 0.004	0.251 ± 0.009
26–28	7.1	0.77 ± 0.10	0.97 ± 0.03	8.53 ± 0.15	0.63 ± 0.03	2.36 ± 0.04	8.28 ± 0.29	0 69 ± 0.04	0.084 ± 0.005	0.285 ± 0.010

cores (PS BC 116, 133, 150, 151; SC QP2; W8709A-1, W8709A-8 and W8709A-13) for the purpose of comparing our results with that of the previous study. Of the cores mentioned above, nine constitute a transect across the Pacific along ~ 40°N, serving to study the effect of offshore gradient in sedimentation rate on scavenging of ^{231}Pa and ^{10}Be.

Cores were also selected to include sediments rich in Mn and Fe oxides, opal and $CaCO_3$, which may help to examine the effect of particle composition on scavenging of the nuclides. Enhanced scavenging of ^{230}Th and ^{231}Pa was suggested to be related to Mn coating of particles in the East Pacific Rise [31] where two cores rich in Mn and Fe were chosen (TT154-10 and V19-55). The major phase scavenging ^{10}Be from water column to the sea floor has been postulated to be aluminosilicate rather than carbonate [6,32]. The relatively high carbonate content in sediments in five cores (V28-238, RC11-210, MANOP Site C, V19-28 and V19-29) along the equator may allow us to test this hypothesis. Scavenging of ^{231}Pa was suggested to be enhanced by high opaline silica flux [33,34]. A role for opal in the scavenging of ^{10}Be has also been inferred from the similarity of Be and Si profiles in sediment pore waters [35]. Since opal is one of the two most important biogenic components (the other being $CaCO_3$) in marine sediments in terms of quantity, the influence of opal flux on scavenging of ^{231}Pa and ^{10}Be is worth close evaluation. In addition to one core in the Bering Sea (RC14-121) where the Holocene sediment contains a very high diatom content [36], we included two cores (E15-6 and E17-9) in the South Pacific (near the Antarctic) where the opal deposition rate is very high [37,38].

The techniques used for analyses of the radionuclides have been described in detail elsewhere [24]. The initial (i.e., decay corrected) unsupported concentrations of ^{230}Th and ^{231}Pa (designated as $^{230}Th_{xs,0}$ and $^{231}Pa_{xs,0}$, respectively; Table 2), were calculated based methods described previously [23,24]. The basic principle of our approach is to use ^{230}Th, a nuclide that is produced uniformly throughout the ocean by decay of dissolved ^{234}U and deposited to the sea floor at a rate nearly equal to its production rate in the overlying water column, as a tracer against which ^{231}Pa and ^{10}Be are normalized so that $^{231}Pa/^{230}Th$ and $^{10}Be/^{230}Th$ ratios in the sediments can be used as indicators of the intensity of scavenging of ^{231}Pa and ^{10}Be (see [23] for a description of the normalization and the assumptions implicit therein; and also discussions in Section 3 below). For the sake of convenience, "Pa/Th" and "Be/Th" will be used throughout the text to designate the ratios of $_{xs}(^{231}Pa/^{230}Th)_0$ and $^{10}Be/^{230}Th_{xs,0}$, respectively.

3. Intensified scavenging of ^{231}Pa and ^{10}Be in ocean margins

The $^{231}Pa/^{230}Th$ production ratio in the water column is known to be a constant value (0.093) because of the fixed ratio of ^{235}U to ^{234}U (the progenitors of ^{231}Pa and ^{230}Th, respectively) in the ocean. Since the rate of removal of ^{230}Th from seawater is relatively uniform throughout the ocean [18,19,22], a Pa/Th ratio in the sediment greater than the production ratio of 0.093 indicates that the site is a sink for ^{231}Pa (relative to ^{230}Th), receiving an extra amount of ^{231}Pa in addition to the ^{231}Pa produced in the overlying water column. Conversely, if the ratio is less than the production ratio, the site acts as a source with a certain fraction of ^{231}Pa produced in the overlying water column being laterally exported (relative to ^{230}Th) to other area(s) in the ocean [23,24]. Similar to Pa/Th ratios, Be/Th ratios can be used as indicators of the intensity of scavenging of ^{10}Be relative to ^{230}Th [23].

Notes to Table 2:

[1] The errors include propagation of 1σ counting statistics. Sources for the ages are given in [26]

[2] The core-top age with a question mark indicates that the mixed layer depth of the core was not known, therefore an age was assigned.

[3] Indicates duplicates of the same sample.

[4] There was not enough BeO for good ^{10}Be measurement due to loss during handling

[5] The samples were taken from different sections at the same depth level, rather than duplicates of the sample.

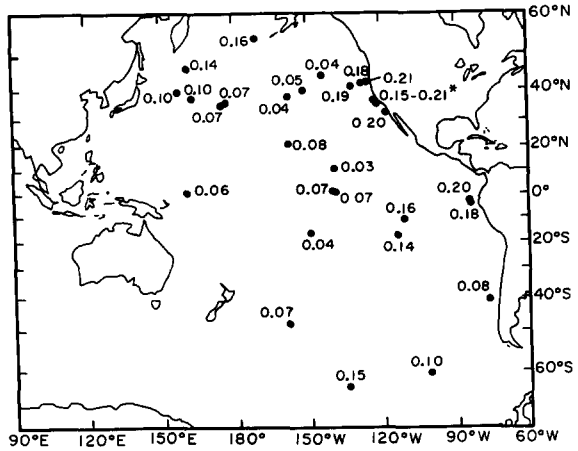

Fig. 2. Average Holocene Pa/Th activity ratios of sediments in the Pacific. Note that there are four cores located in the coastal area off California. The range of the Pa/Th ratios (marked with an asterisk) is from 0.15 to 0.21, excluding the exceptionally high Pa/Th ratio of PS BC 133 (see text for explanation).

For most of the cores, two samples were taken from the Holocene section for the radiochemical analysis. Where this is the case the averages of the two Pa/Th and Be/Th ratios are used to represent the Holocene results. As will be demonstrated below, the overall results indicate that both ^{231}Pa and ^{10}Be are preferentially removed to sediments in ocean margin regions (as shown by higher Pa/Th and Be/Th ratios), i.e., boundary scavenging has a great influence on removal of these two nuclides from the ocean.

The lowest Pa/Th ratio (0.03) among the open ocean sites is at MANOP Site S whose sedimentation rate is < 0.1 cm/ky [39]; the Pa/Th ratios in some margin areas are around 0.2 (Fig. 2): two times higher than the production ratio, clearly showing a pattern of boundary scavenging. On average, the Pa/Th ratio in ocean margin sediments (~ 0.15 to 0.2) is about 4–5 times that in areas of red clay accumulation in the open ocean (~ 0.03–0.04). The pattern of boundary scavenging of ^{231}Pa (relative to ^{230}Th) in this study is in agreement with published results summarized in [20] and our data fill in the Eastern Pacific where some of the ^{231}Pa concentrations in [20] were inferred.

Similarly, the pattern of boundary scavenging of ^{10}Be is shown by higher Be/Th ratios in margin sediments (Fig. 3). The very low Be/Th ratios in the pelagic sediment in the open ocean in this study are in agreement with the Be/Th ratios measured by other investigators in the same type of sediment (see + symbols in Fig. 3). The lowest Be/Th ratio (0.03×10^9 atoms/dpm) in this study is also at MANOP Site S. In margin areas, the Be/Th ratios range from 0.3 to 1.5×10^9 atoms/dpm. The range in the Be/Th ratio between ocean margin sediments and deep open ocean red clay sediments exceeds a factor of 10, i.e., approximately twice the range seen for Pa/Th ratios.

One core (PS BC133 from the coastal area of California) has exceptionally high ratios of Pa/Th (average 0.85) and Be/Th (average 14.2×10^9 atoms/dpm; Table 2). The very high contents of Fe and K (20% and 4.2%, respectively [26]) of this core suggest that the samples from this core might be rich in glauconite, a mineral that usually forms in shallow margin areas [40] and has been reported to be present in sandy sediments in this area, with a maximum concentration of 35% of the total sediments [41]. Since such a result is so rare in our data set, we do not consider it representative of average ocean margin environments, but it apparently suggests the preferential uptake of ^{10}Be and ^{231}Pa, relative to ^{230}Th, by the Fe-rich minerals in these sediments.

The generally higher Pa/Th and Be/Th ratios in the ocean margin cores compared to the open

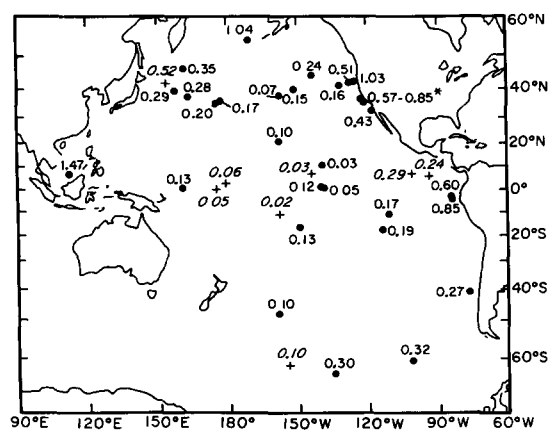

Fig. 3 Average Holocene Be/Th ratios (10^9 atoms/dpm) of sediments in the Pacific. Note that there are four cores located in the coastal area off California. The range of the Be/Th ratios (marked with an asterisk) does not include that of PS BC133 (see text). Also shown are the Be/Th ratios taken from published literature (the sites marked with +).

ocean cores may be more easily seen in Fig. 4, in that the cores are so arranged that those in the upper part of the figure are from open ocean areas (i.e., sedimentation rates are relatively low) and those in the lower part are from margins (i.e., sedimentation rates are relatively high). A general correlation is seen between sedimentation rate and the Pa/Th ratio (Fig. 4a), and between sedimentation rate and the Be/Th ratio (Fig. 4b). Also shown in the figure are the ratios of Be/Th normalized to water depth ($[Be/Th]_N$; Fig. 4b). The vertical distribution of dissolved ^{10}Be in the open Pacific exhibits a depletion in surface waters (~ 600–1000 atoms/g) and enrichment to relatively constant values at depth (~ 2000 atoms/g), which is suggested to reflect scavenging of ^{10}Be from the surface waters followed by regeneration at depth [42]. The production of ^{230}Th is directly proportional to water depth and the source of ^{230}Th is, therefore, greater at deeper sites. Consequently, if ^{230}Th is removed throughout the water column [18,19,24] and ^{10}Be is only removed from surface waters [42], then, among the sites of similar scavenging intensity, the Be/Th ratios of sediments in shallow ocean areas will be higher than that in deep ocean areas. For the purpose of comparing ^{10}Be scavenging rates at different sites in the ocean, Be/Th ratios should, therefore, be normalized to a constant water depth. The mean depth of 4200 m of the Pacific [43] was chosen against which the Be/Th ratios were normalized:

$$[Be/Th]_N = (Be/Th) \times Z/4200 \quad (1)$$

where (Be/Th) is the measured ratio and Z is the water depth (in meters) above the core. Normalization of the Be/Th ratio to a standard water depth leads to a minimum estimate for the extent to which ^{10}Be is influenced by boundary scavenging. Implicit in this approach is the assumption that ^{10}Be is scavenged only from surface waters [42]. This may not be valid in ocean

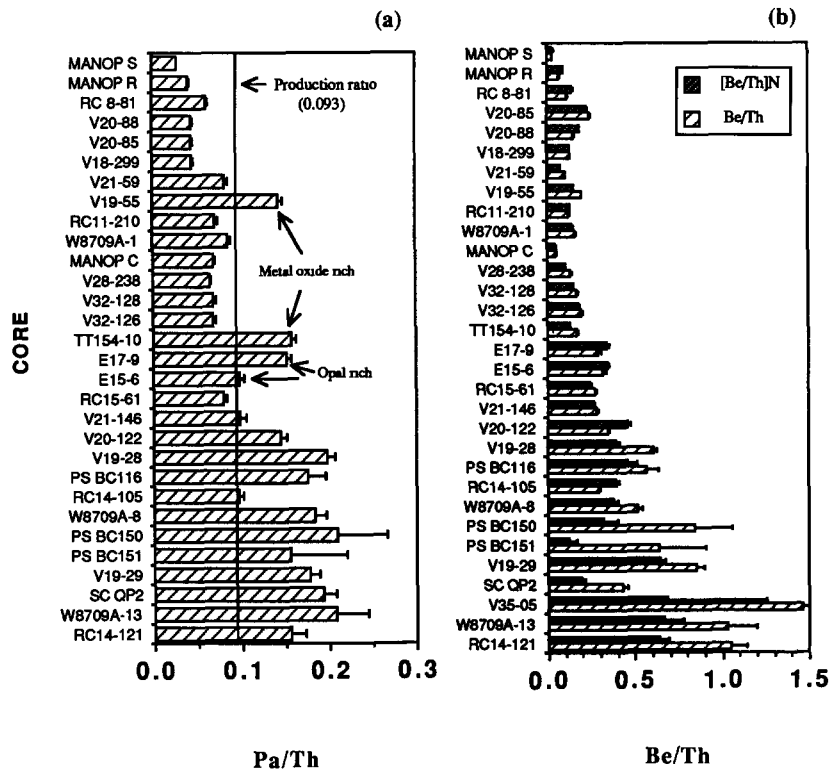

Fig. 4. (a) Average Holocene Pa/Th activity ratios versus cores. (b) Average Be/Th ratios (10^9 atoms/dpm) versus cores. The cores are so arranged that the sedimentation rate is low at the top and high at the bottom of the figure. Also shown in (b) are the depth-normalized Be/Th ratios (i.e., $[Be/Th]_N = (Be/Th) \times Z/4200$, where Z is the water depth of the cores in meters and 4200 is the mean depth of the Pacific adopted from [43]). The results of PS BC133 are not included (see text).

margin regions where fluxes of ^{10}Be collected by sediment traps indicate that scavenging takes place throughout the water column [24], in which case the depth normalization will underestimate the actual enhancement of ^{10}Be deposition. Another factor which causes estimates of the extent of boundary scavenging of ^{231}Pa and ^{10}Be, based on Pa/Th and Be/Th ratios, to be minimum values is the assumption that the deposition rate of ^{230}Th is everywhere equal to its production rate in the overlying water column. Boundary scavenging also exerts some influence on ^{230}Th [24], so that the actual enhancement of the deposition of ^{231}Pa and ^{10}Be in ocean margin sediments should be obtained by multiplying the Pa/Th and Be/Th ratios by the extent to which ^{230}Th deposition is enhanced at margins (note that enhancement of ^{230}Th deposition at margins is generally unknown; see modeling results in Section 5). Yet, despite these conditions, which lead to minimum estimates of enhanced scavenging at margins, the depth normalized Be/Th ratios ($[Be/Th]_N$) still span a full order of magnitude (Fig. 4b), providing unequivocal evidence for greatly enhanced scavenging of ^{10}Be in ocean margin areas.

4. Factors influencing scavenging

A regional study in the Northeastern Pacific found that fluxes of ^{230}Th, ^{231}Pa and ^{10}Be are proportional to particle flux, both with respect to temporal variability at a single location and with respect to mean particle flux along a transect normal to the coastline [24]. It remains to be tested, however, if a general relationship exists between the nuclide scavenging rate and particle flux on a basin-wide scale.

Nine cores (core sites 3, 4, 5, 6, 7, 8, 10, 11, and 12, Fig. 1) along a transect across the North Pacific at ~40°N provide a useful subset with which to test the influence of particle flux on scavenging intensity on a basin-wide scale. Sediments across the North Pacific are predominantly lithgenic material transported by westerly winds from source regions in Asia [27,28]. Dust flux, and hence sediment accumulation rate, generally decreases from west to east in the open ocean. As there is no information on particle flux in the water column at the sites where the cores in this

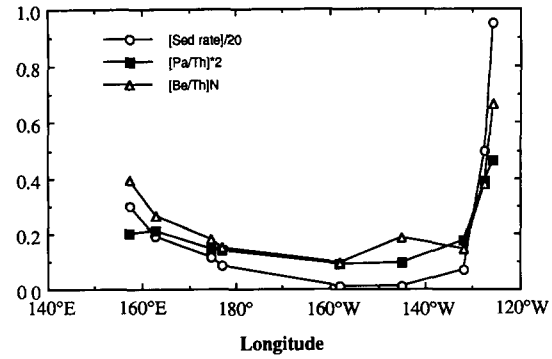

Fig. 5. Sediment accumulation rates (cm/kyr), and average Holocene ratios of Pa/Th (activity ratio) and $[Be/Th]_N$ (10^9 atoms/dpm) for nine cores along ~40°N transect in the North Pacific.

study were collected, sedimentation rates may be regarded as the best proxy. Patterns of Pa/Th and $[Be/Th]_N$ ratios both closely mimic the pattern of sedimentation rate along the 40°N transect (Fig. 5). As has been discussed previously, Pa/Th and $[Be/Th]_N$ ratios vary according to the scavenging intensities of ^{231}Pa and ^{10}Be. Therefore the close relationships between sedimentation rate and Pa/Th and $[Be/Th]_N$ ratios suggest that particle flux is a major factor influencing scavenging of ^{231}Pa and ^{10}Be, consistent with the findings of an earlier study of ^{10}Be by Tanaka et al. [44]. However, there are exceptions when the results of all the cores are considered. The deviation from the correlation between sedimentation rate and the Pa/Th and $[Be/Th]_N$ ratios could be partly due to errors in the sedimentation rates of the cores, which are difficult to assess at the moment because the chronologies of these cores are mostly taken from literature. Sediment composition, which varies among cores, may also affect the scavenging intensity (Fig. 4).

Principal component analysis was applied to the elemental results of the sediments (the element concentrations and mathematical procedures were given in [26]) to look for systematic relationships between sediment composition and the nuclide contents. The factor analysis results indicate that the elements may be divided into three groups (Fig. 6):

(1) those normally associated with lithogenic phases (Al, Ti, Fe, K, Mg, V and ^{232}Th);

(2) those associated with biogenic carbonates (Ca, Sr and Zn);

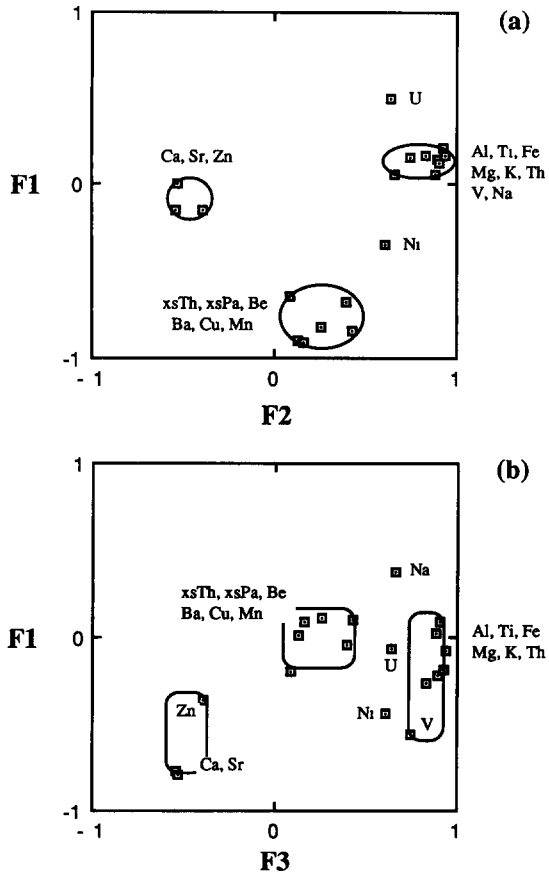

Fig. 6. Two-dimensional plots of the first three extracted components (F_1, F_2 and F_3) based on principal component analysis applied to the elemental data in this study (details given in [26]). (a) F_1 vs F_2. (b) F_1 vs F_3. The first extracted component (F_1) accounts for 41%, the second (F_2) 24% and the third (F_3) 12%, of the total variance. With the sum of the three components (F_1, F_2 and F_3) accounting for 77% of the total variance, most of the interesting information can therefore be found in these three components. Note that not included for principal component analysis were the elmental results of PS BC133 (from coastal California) which contains very high Fe and K contents and TT154-10 and V19-55 (from the East Pacific Rise), which are very rich in Fe and Mn oxides (see text).

(3) ^{230}Th, ^{231}Pa, ^{10}Be (designated by $_{xs}$Th, $_{xs}$Pa and Be), Ba, Cu and Mn.

In a broader sense, Na, Ni and U seem to be clustered around the lithogenic elements. ^{230}Th, ^{231}Pa and ^{10}Be are located far away from Ca and Sr in Fig. 6, which is consistent with the hypothesis that marine carbonates may act as diluting phases and do not contribute significantly to nuclide scavenging [6,32]. Distributions of some trace elements (i.e., Ba, Cu and Mn) may be related to biological productivity, albeit for different reasons. Diagenetic enrichment of Mn in sediments usually occurs in areas of high biological productivity where organic input to the sediments is high (e.g., in the Northeastern Pacific; [24,45]). Cu chemistry in the ocean seems to be substantially influenced, and often dominated, by organic complexation [46,47]. The sedimentary distribution of Ba, an element known to be associated with biogenic opal [48], has been proposed as a paleoproductivity indicator [e.g., 49,50]. The association of Ba with ^{230}Th, ^{231}Pa, ^{10}Be, Cu and Mn (Fig. 6) therefore suggests that scavenging of these nuclides and elements may be related to biological productivity in surface waters.

Comparing results from two end member locations supports the inferences based on factor analysis. Two cores from the South Pacific (E15-6 and E17-9) very rich in opal content (60–80%; [37,38]) serve as an end member to examine the effect of opal flux on scavenging of ^{231}Pa and ^{10}Be. MANOP Site R in the central North Pacific is treated here as a pure red clay end member. The average concentrations of initial unsupported ^{231}Pa and ^{10}Be (~ 3.4 dpm/g and $\sim 5.7 \times 10^9$ atoms/g, respectively) in MANOP Site R are close to those (~ 2.4 dpm/g and $\sim 6.0 \times 10^9$ atoms/g, respectively) in E15-6 and E17-9 (Table 2). The sedimentation rate of E15-6 and E17-9 (~ 3.6 cm/ky) is more than one order of magnitude higher than that of MANOP Site R (~ 0.2 cm/ky). Therefore, accumulation rates of ^{231}Pa and ^{10}Be in the opal-rich sediments of the South Pacific must be more than 10 times their respective accumulation rates in the red clay sediment of MANOP Site R in the central North Pacific, leading us to conclude that opal, as well as clay minerals, must be an important phase scavenging ^{231}Pa and ^{10}Be.

5. Modeling distributions of ^{231}Pa and ^{10}Be

One of our goals is to evaluate an ocean-wide ^{10}Be deposition rate which, in turn, provides an estimate of global average production rate of ^{10}Be in the atmosphere. It has been demonstrated above (also see [23,24]) that the removal of ^{231}Pa and ^{10}Be is greatly influenced by boundary scavenging. Furthermore, lateral sediment

transport (sediment focussing) can result in misinterpretation of ^{231}Pa and ^{10}Be fluxes in sediments [23]. Therefore, one can not reliably determine the ocean-wide ^{10}Be deposition rate by measuring its accumulation rate in only a few cores. A better approach is to develop a model that relates the burial of ^{10}Be to the burial of ^{230}Th, whose source is precisely known. In the following, a simple boundary scavenging box model is constructed and the validity of input parameters is first tested using ^{230}Th and ^{231}Pa results.

5.1. ^{231}Pa

If the deposition rate of ^{230}Th in sediments is exactly equal to its production in the water column, then the flux of nuclide N at a specific site, F(N), could be evaluated as [23,51,52]:

$$F(\mathrm{N}) = [\mathrm{N/Th}]_{sed} \times P_{Th} \qquad (2)$$

where $[\mathrm{N/Th}]_{\mathrm{sed}}$ is the concentration ratio of nuclide N to the initial unsupported ^{230}Th in the sediment; P_{Th} is the production rate of ^{230}Th which is proportional to water depth (i.e., $P_{\mathrm{Th}} = 0.0026Z$ dpm/cm^2 ky^{-1}, where depth, Z, is in meters). However, $F(^{230}\mathrm{Th})$ is not equal to P_{Th} in the real world because boundary scavenging can to some extent affect ^{230}Th [22,24]. Since the mass budgets of ^{231}Pa and ^{10}Be will be constructed by normalizing to ^{230}Th, the boundary scavenging effect on ^{230}Th must be taken into account. A model will have to be constructed in which open ocean and ocean margin regions are both considered (Fig. 7). When the two-box system is at steady state, the ^{230}Th deposited in margin sediment is derived both from that produced in the overlying water column, and from that imported from the open ocean. This mass balance requires:

$$Q_m^i + (1 - K_o) \times Q_o^i - K_m \times Q_m^i = 0 \qquad (3)$$

Rearranging:

$$K_m = 1 + (1 - K_o) \times \left(\frac{Q_o^i}{Q_m^i} \right) \qquad (4)$$

where $Q_{\mathrm{o}}^{\mathrm{i}}$ ($= P_{\mathrm{Th}} \times V_{\mathrm{o}}$) and $Q_{\mathrm{m}}^{\mathrm{i}}$ ($= P_{\mathrm{Th}} \times V_{\mathrm{m}}$) are the rates of in situ production of ^{230}Th (in units of dpm/yr) in the open ocean and ocean margin

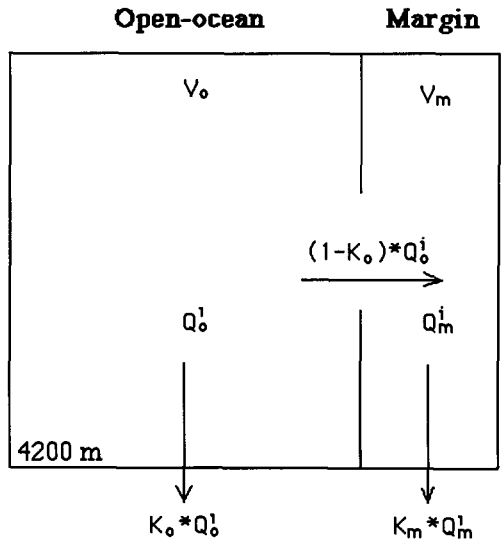

Fig. 7. A two-box model illustrating boundary scavenging in the Pacific. The mean depth of 4200 m is from [43]. o = open ocean; m = margin; V = volume of the ocean; Q^{i} = rate of in situ production of ^{230}Th (dpm/yr); K_{o} = percentage of ^{230}Th produced in the open ocean that is directly removed in the open ocean, K_{m} = enrichment factor for ^{230}Th in the margin sediemnts (see text).

boxes, respectively (with V_{o} and V_{m} referring to the open ocean volume and ocean margin volume in m^3); K_{o} is the percentage of ^{230}Th produced in the open ocean box that is directly deposited over the open ocean floor; K_{m} is the enrichment factor for ^{230}Th deposition in margin sediment due to boundary scavenging (it can be regarded as the ratio of actual flux of ^{230}Th to the margin sediment relative to the production of ^{230}Th in the overlying ocean margin water column).

Equation (4) can be rewritten as:

$$K_m = 1 + (1 - K_o) \times \left[\frac{(1 - f_m)}{f_m} \right] \qquad (5)$$

where $f_{\mathrm{m}} = V_{\mathrm{m}}/(V_{\mathrm{o}} + V_{\mathrm{m}})$ is the ocean margin volume fraction.

Assuming that any ^{230}Th and ^{231}Pa which are not scavenged from the open-ocean box are transported to the ocean margin box where they are homogeneously mixed with the ^{230}Th and ^{231}Pa produced in the waters in the ocean margin box, and then scavenged to the margin sediment, we then have:

$$[\mathrm{Pa/Th}]_{\mathrm{o}} \times K_{\mathrm{o}} \times (1 - f_{\mathrm{m}}) + [\mathrm{Pa/Th}]_{\mathrm{m}} \times \mathrm{K_m} \times \mathrm{f_m} = 0.093 \qquad (6)$$

where $[Pa/Th]_o$ and $[Pa/Th]_m$ are the initial unsupported $^{231}Pa/^{230}Th$ ratios of representative open ocean and ocean margin sediments, respectively; 0.093 is the constant water column $^{231}Pa/^{230}Th$ production ratio.

In modeling the scavenging of ^{230}Th, K_o is first permitted to range from 0.85 to 0.95 based on modeling results in [22], and K_m is calculated using eqn. (5), assuming that the fraction of the ocean margin volume is 10% of the total Pacific Ocean (i.e., $f_m = 0.1$). The computed K_m values range from 1.45 to 2.35 (Table 3), very close to the flux/production ratio for ^{230}Th (i.e., the observed K_m) for sediment trap samples and Holocene sediments (from 1.7 to 2.5) at a nearshore site in the Northeastern Pacific [24]. Thus, the assumed values for K_o (0.85–0.95) lead to computed K_m values that are consistent with the best estimates of K_m available from measured ^{230}Th fluxes.

To test the parameters used to simulate boundary scavenging, an average value for $[Pa/Th]_m$ of 0.2 was used as model input based on the facts that the Pa/Th ratios in sediment trap samples from a nearshore site in the Northeastern Pacific are around 0.2 [24], and those in the margin sediments are relatively constant (~ 0.2; Fig. 4a). Equation (6) was then used to compute values of $[Pa/Th]_o$ over the permitted range of K_o, giving values (0.060–0.075), consistent with the range of the observed Pa/Th ratios (i.e., from 0.03 to 0.09) in the open ocean sediments (Fig. 2). The parameters used (i.e., $f_m = 0.1$, $K_o = 0.85$–0.95, and $K_m = 1.45$–2.35; Table 3) thus give a reasonable partitioning of ^{230}Th and ^{231}Pa between open ocean and ocean margin sediments, and will therefore be used for modeling the distribution of ^{10}Be.

5.2. ^{10}Be

The Pacific ocean-wide average ^{10}Be flux (F_{Be}) in the two-box model (Fig. 7) is given by:

$$F_{Be} = P_{Th} \times \{({}_o[Be/Th]_N) \times K_o \times (1 - f_m) + ({}_m[Be/Th]_N) \times K_m \times f_m\} \quad (7)$$

where P_{Th} is the average ^{230}Th production rate in the Pacific ($= 0.0026 \times 4200$ dpm/cm^2 ky^{-1}); ${}_o[Be/Th]_N$ and ${}_m[Be/Th]_N$ refer to the depth-normalized Be/Th ratios in the open ocean and ocean margin box, respectively.

Representative ratios of ${}_o[Be/Th]_N$ and ${}_m[Be/Th]_N$ must be chosen in order to obtain an average ^{10}Be flux (F_{Be}) in the Pacific. Since a vast area of deep open Pacific is covered by pelagic (red clay) sediment whose accumulation rate is very low (~ 1 mm/ky), and the Be/Th ratio for red clay in the open ocean is from about 0.02 to 0.10×10^9 atoms/dpm (Fig. 3), our present best estimate of the ${}_o[Be/Th]_N$ ratio for *average open ocean sediments* falls between 0.04 and $0.06 \times^9$ atoms/dpm. Excluding some extreme values, the

TABLE 3

Modeling results of ^{231}Pa in the Pacific Ocean [a]

Model input			Model output	
f_m	K_o [b]	$[Pa/Th]_m$	K_m [c]	$[Pa/Th]_o$ [d]
0.1	0.80	0.2	2.80	0.051
0.1	0.85	0.2	2.35	0.060
0.1	0.90	0.2	1 90	0.068
0.1	0.95	0.2	1.45	0.075
0.1	1.00	0.2	1.00	0.081

[a] This is a simple mass budget constraint on the ocean-wide production and removal of ^{230}Th and ^{231}Pa. The ocean margin volume fraction (f_m) is assumed to be 0.1 and the representative Pa/Th ratio in the margin sediment ($[Pa/Th]_m$) is taken to be 0.2 (see text).

[b] K_o is the percentage of the ^{230}Th produced in the open ocean that is directly deposited over the open ocean floor based on the modelling results of Bacon [22] and constraints by the measured ^{230}Th fluxes in the sediment traps and sediments in the Northeastern Pacific [24].

[c] K_m is the enrichment factor of ^{230}Th in the margin ocean sediment (i.e., the ratio of actual flux to the production rate in the overlying water column) calculated using eqn. (5).

[d] $[Pa/Th]_o$ is the average Pa/Th ratio for the open ocean sediment calculated using eqn. (6).

TABLE 4

Model computations of the ocean wide average ^{10}Be deposition rate (F_{Be}) as well as the fraction of total ^{10}Be deposited in margin sediments of the Pacific Ocean [1]

K_o	K_m	F_{Be} (10^9 atoms/cm^2 kyr^{-1})	^{10}Be deposited in margin sediment [2] (%)
Lower limit for F_{Be} using ${}_o[Be/Th]_N = 0.04 \times 10^9$ and ${}_m[Be/Th]_N = 0.4 \times 10^9$ atoms/dpm			
0 80	2.80	1.54	80
0.85	2.35	1.36	75
0.90	1 90	1.18	70
0.95	1.45	1.01	63
1 00	1.00	0.83	53
Upper limit for F_{Be} using ${}_o[Be/Th]_N = 0\ 06 \times 10^9$ and ${}_m[Be/Th]_N = 0.6 \times 10^9$ atoms/dpm			
0.80	2.80	2.31	80
0 85	2.35	2.04	75
0.90	1 90	1.77	70
0.95	1.45	1.51	63
1.00	1.00	1.24	53

[1] K_o and K_m are the same as in Table 3. The mean depth of the Pacific Ocean is taken to be 4200 m [43]. The ocean margin volume fraction (f_m) is assumed to be 0.1. ${}_o[Be/Th]_N$ and ${}_m[Be/Th]_N$ are the average Be/Th ratios in the open ocean and ocean margin sediments, respectively. F_{Be} is calculated using eqn. (7) (see text).

[2] This is calculated as $(P_{Th} \times ({}_m[Be/Th]_N) \times K_m \times f_m)/F_{Be}$. See eqn. (7) for explanations of the parameters.

${}_m[Be/Th]_N$ ratio for *average ocean margin sediments* falls between 0.4 and 0.6×10^9 atoms/dpm (Fig. 4b). For the chosen f_m, K_o and K_m values (obtained from modeling of ^{231}Pa), and the upper and lower limits for ${}_o[Be/Th]_N$ and ${}_m[Be/Th]_N$ ratios defined above, a series of results (Table 4) for the average flux of ^{10}Be in the Pacific (F_{Be}) can be obtained based on eqn. (7). Although F_{Be} obviously depends on the modeling parameters chosen, we can still place some limits on it. If we assume some extreme parameters, we can obtain a lower limit of $1.0 \times^6$ atoms/cm^2 yr^{-1} (with $K_o = 0.95$; ${}_o[Be/Th]_N$ and ${}_m[Be/Th]_N$ ratios of $0.04 \times^9$ and 0.4×10^9 atoms/dpm, respectively), and an upper limit of 2.0×10^6 atoms/cm^2 yr^{-1} (with $K_o = 0.85$; ${}_o[Be/Th]_N$ and ${}_m[Be/Th]_N$ ratios of 0.06×10^9 and 0.6×10^9 atoms/dpm, respectively) (Fig. 8). Therefore, our best estimate of F_{Be} is $(1.5 \pm 0.5) \times 10^6$ atoms/cm^2 yr^{-1} (i.e., the average of the two extreme limits above). If we assume some moderate values for the modeling parameters (i.e., a K_o of 0.9; ${}_o[Be/Th]_N$ and ${}_m[Be/Th]_N$ ratios of 0.05×10^9 atoms/dpm and 0.5×10^9 atoms/dpm, respectively), then F_{Be} is also 1.5×10^6 atoms/cm^2 yr^{-1}; and ~70% of the ^{10}Be supplied to the Pacific is accumulated in ocean margin sediment underlying only 10% of the total Pacific Ocean volume (Table 4).

Since this is a Pacific-wide study, and factors such as boundary scavenging and sediment focusing that influence the deposition of ^{10}Be in the ocean have been taken into account, the average Holocene ^{10}Be flux in the Pacific should reflect the global average production rate of ^{10}Be in the atmosphere during the Holocene period. However, before such a conclusion is reached, possible exchanges of ^{10}Be between the Pacific and the Atlantic need to be considered in terms of the regional residence times of ^{10}Be and the way of water exchange between oceans.

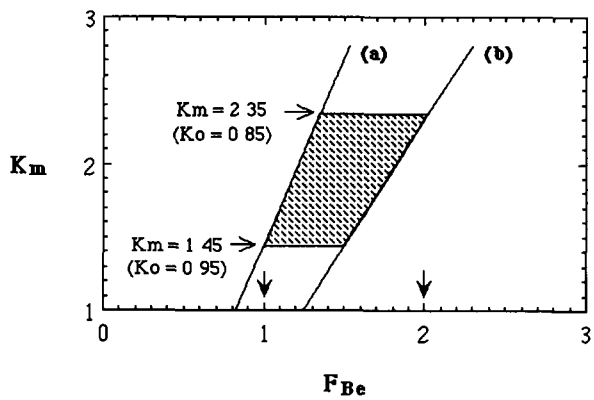

Fig. 8. Modelled relationships between the ocean-wide average accumulation rate of ^{10}Be in the Pacific Ocean (F_{Be}) and the enhancement of ^{230}Th deposition in ocean margin sediments (K_m). The volume fraction of ocean margin and the mean depth of the ocean are assumed to be 10% and 4200 m, respectively. The hatched area is constrained by the permitted range of values for the parameters used to define K_m (eqn. (5)), and the relationship between K_m and F_{Be} (eqn. (7)). a = the relationship between K_m and F_{Be} for lower-limit values of Be/Th ratios in open ocean and ocean margin sediments ($0\ 04 \times 10^9$ atoms/dpm and 0.4×10^9 atoms/dpm, respectively). b = the same relationship for upper-limit values of Be/Th ratios in open ocean and ocean margin sediments (0.06×10^9 atoms/dpm and 0.6×10^9 atoms/dpm, respectively). The lower and upper limits for F_{Be} permitted by the extreme ranges of reasonable values for the parameters are $1\ 0 \times 10^6$ atoms/cm^2 yr^{-1}, and 2.0×10^6 atoms/cm^2 yr^{-1}, respectively, as indicated by the solid arrows.

5.3. *Regional residence times of ^{10}Be*

The oceanic residence time of ^{10}Be is an important index for estimating the rate of removal of ^{10}Be in the ocean. The residence time (τ) with respect to removal from seawater may be calculated using the following equation [23]:

$$\tau = I/F(\mathrm{Be}) \quad (8)$$

where I is the inventory of ^{10}Be in the ocean (in the unit of atoms/cm^2) and is simply proportional to water depth if we adopt a mean ^{10}Be concentration in the deep Pacific ($\sim$ 1800 atoms/g [42]); F(Be) is the ^{10}Be deposition rate (atoms/cm^2 yr^{-1}) at a specific site as defined in eqn. (2).

The regional residence times of ^{10}Be thus calculated do not take into account the effect of boundary scavenging on ^{230}Th because there is no independent assessment of the effect of boundary scavenging of ^{230}Th at individual sites. However, since we know that a certain fraction (e.g., $\sim$ 10%) of ^{230}Th produced in the open ocean is removed to the margins, ^{10}Be residence times calculated for open ocean areas should be regarded as lower limits (because the deposition rates of ^{10}Be are upper limits using eqn. (2)); and those in ocean margin areas should be upper limits (because the deposition rates of ^{10}Be are lower limits). The residence time of ^{10}Be ranges from < 100 yr in ocean margin areas to > 1000 yr in deep, open ocean with very low accumulation rates (Fig. 9). The trend is obvious: residence times in open ocean regions are generally longer and those in margin areas are shorter, with the latter being at least an order of magnitude lower than the former, which is a consequence of intensified scavenging in ocean margin areas.

Although the ^{10}Be residence time varies greatly from area to area in the Pacific, an average ^{10}Be residence time is useful in evaluating the behavior of ^{10}Be in the ocean. Using an average ^{10}Be flux of 1.5×10^6 atoms/cm^2 yr^{-1} calculated from the above modeling, a mean ^{10}Be concentration of 1800 atoms/g [42] and a mean depth of the Pacific of 4200 m [43], the calculated mean ^{10}Be residence time in the Pacific is $\sim$ 500 yr, consistent with the recent estimate of Kusakabe et al. [53]. The residence time of ^{10}Be in the open deep Atlantic is $\sim$ 500 yr [54], about half of that ($\sim$ 1000 yr) in the open deep Pacific. By analogy to the mean residence time of ^{10}Be in the Pacific, the mean residence time of ^{10}Be in the Atlantic may be shorter than 250 yr (i.e., less half of the residence time of the open deep Atlantic), which is much less than the inter-ocean mixing time ($\sim$ 1000 yr). Considering the short residence times of ^{10}Be ($\sim$ 250 yr) in the South Pacific (Fig. 9) and in the Atlantic, the net change in the inventory of ^{10}Be due to transport of ^{10}Be between the Atlantic and the Pacific is expected to be small because of the effects of high scavenging intensity in the South Pacific and a larger influence of boundary scavenging in the smaller Atlantic compared to the Pacific.

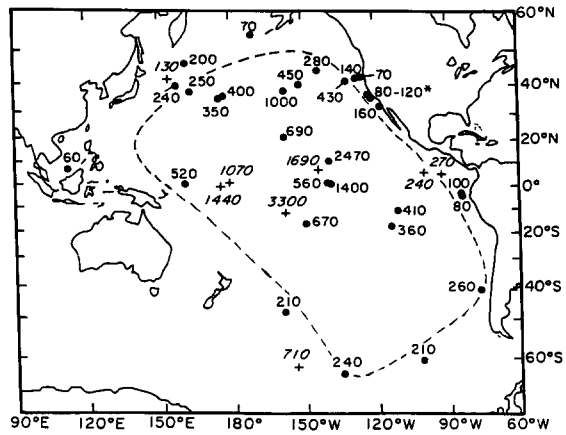

Fig. 9. Regional residence times (years) of ^{10}Be in the Pacific. + = values based on literature results. The dashed line is drawn by eye indicating an isoline of a residence time of 250 yr.

Another cause of the small partitioning of ^{10}Be between the Pacific and the Atlantic is the way of water exchange between the Pacific and the Atlantic. The advection flow is from surface North Atlantic to deep North Atlantic to Antarctic Circumpolar Currents to deep Pacific and to surface Pacific, and the surface Pacific water is exported to the Indian Ocean via the Indonesian Seas, and then around the southwest of Africa, into South Atlantic Ocean [55]. Considering that the ^{10}Be concentration in the surface Pacific water ($\sim$ 850 atoms/g [42]) is about the same as that in the deep Atlantic [54], mixing and exchange between the Atlantic and the Pacific oceans is unlikely to influence the partitioning of ^{10}Be between the two oceans significantly. This

suggests that the Pacific acts as a relatively closed basin with respect to ^{10}Be supplied from the atmosphere and the average flux of ^{10}Be in the Pacific can be regarded as a good estimate of the global average production rate of ^{10}Be.

6. Conclusions

Boundary scavenging plays an important role in removal from the ocean of both ^{231}Pa and ^{10}Be. Particle flux appears to be the major factor influencing scavenging of ^{231}Pa and ^{10}Be in the ocean. Principal component analysis of the chemical data suggests that biological opal productivity may also influence scavenging of ^{231}Pa and ^{10}Be. Modeling results indicate that about 70% of the ^{10}Be directly supplied to the ocean from the atmosphere is accumulated in sediments in ocean margins, which constitute only 10% of the total Pacific volume. The regional residence times of ^{10}Be in the Pacific range from < 100 yr in margin areas to > 1000 yr in the deep open ocean, with a mean residence time of ~ 500 yr.

The results of the modeling allow us to place the lower and upper limits for the range of the global average production rate of ^{10}Be at 1.0×10^6 atoms/cm^2 yr^{-1} and 2.0×10^6 atoms/cm^2 yr^{-1}, respectively, averaging $(1.5 \pm 0.5) \times 10^6$ atoms/cm^2 yr^{-1}.

The results of this study have several important implications:

(1) ^{10}Be has been used to trace the cycling of ocean floor sediments at convergent tectonic plates (island arc volcanic rocks; e.g., [56,57]). The influence of boundary scavenging on the deposition of ^{10}Be in the specific areas of the ocean margins should be well understood before ^{10}Be can be used to model the amount of sediment that was incorporated in the magmatic process accurately.

(2) The production rate of ^{10}Be in the atmosphere reflects the intensity of the cosmic ray flux and the strength of the Earth's magnetic field. The approach described in this paper can be used to detect changes in ^{10}Be production rate [58], from which information about cosmic ray flux and magnetic field strength in the past may be inferred.

(3) Application of ^{10}Be and ^{231}Pa to dating deep-sea sediments requires a knowledge of the source, transport and fate of ^{10}Be and ^{231}Pa in the ocean. Possible changes in the nature and intensity of boundary scavenging of ^{10}Be and ^{231}Pa may cause changes in deposition rates of ^{10}Be and ^{231}Pa in deep-sea sediments at specific sites, thereby invalidating the assumption of a steady supply of ^{10}Be and ^{231}Pa with time to the sediments. This assumption needs to be examined before a precise chronology can be developed for deep-sea cores based on measurements of ^{10}Be and ^{231}Pa.

Acknowledgements

The authors wish to thank Marty Fleischer, Ginger Eberhart and Jim Wright for their laboratory assistance. Discussions with Jim Hays, Joe Morley, Lloyd Burckle, Flip Froelich, Connie Sancetta and Mitch Lyle (all at Lamont) were very helpful in selecting sediment samples for this study. Most of the samples were taken from the LDGO Deep-Sea Sample Repository (supported by the NSF through Grant OCE88-00001 and the ONR through Grant N00014-87-K-0204). The Multitracers sediments were supplied by the Oregon State University Core Repository (under the NSF Grant OCE88-00458). Samples from two cores in the South Pacific Ocean were provided by the Antarctic Core Library of Florida State University (supported by the NSF's Division of Polar Programs). Marilyn R.B. Ten Brink is thanked for providing sediments from MANOP Sites R and S. Clare Reimers is acknowledged for providing unpublished results on sedimentation rates of several cores in the coastal California area. We are very grateful to John Edmond and Julie Morris for their critical reviews which improved the manuscript considerably. This research was supported by the NSF grant OCE 89-11427. This is Columbia University LDGO contribution 4953.

References

1 D. Lal and B. Peters, Cosmic ray produced radioactivity on the earth, in: Encyclopedia of Physics, Vol 46/2, 551–612, Springer, New York, 1967.

2 M.C. Monaghan, S. Krishnaswami and K.K. Turekian, The global average production rate of ^{10}Be, Earth Planet. Sci. Lett. 76, 279–287, 1986.

3 B.L K Somayajulu, Analysis of causes for the beryllium-10 variations in deep sea sediments, Geochim Cosmochim. Acta 41, 909–913, 1977.
4 S. Tanaka, T Inoue and M. Imamura, The ^{10}Be method of dating marine sediments—comparison with the paleomagnetic method, Earth Planet. Sci. Lett. 37, 55–60, 1977.
5 S. Tanaka and T. Inoue, ^{10}Be dating of North Pacific sediment cores up to 2.5 million years B P , Earth Planet. Sci Lett. 45, 181–187, 1979
6 J.R. Southon, T.-L Ku, D.E. Nelson, J.L Reyss, J.C. Duplessy and J.S. Vogel, ^{10}Be in a deep-sea core: implications regarding ^{10}Be production changes over the past 420 ka, Earth Planet. Sci. Lett. 85, 356–364, 1987.
7 W.U. Henken-Mellies, J. Beer, F. Heller, K J Hsu, C. Shen, G. Bonani, H.J. Hofmann, M. Suter and W. Wolfli, ^{10}Be and ^{9}Be in South Atlantic DSDP Site 519· relation to geomagnetic reversals and to sediment composition, Earth Planet. Sci Lett. 98, 267–276, 1990.
8 A. Mangini, M. Segl, G. Bonani, H.J Hofmann, E. Morenzoni, M. Nessi, M. Suter, W. Wolfli and K K. Turekian, Mass spectrometric ^{10}Be dating of deep-sea sediments applying the Zurich tandem accelerator, Nucl. Instr. Methods Phys. Res. B5, 353–358, 1984
9 L. Brown, J. Klein and R. Middleton, Anomalous isotopic concentrations in the sea off Southern California, Geochim. Cosmochim. Acta 49, 153–157, 1985.
10 A Eisenhauer, A. Mangini, M Segl, J. Beer, G. Bonani, M. Suter and W. Wolfli, High resolution ^{10}Be and ^{230}Th profiles in DSDP Site 580, Nucl Instr. Methods Phys Res. B29, 326–331, 1987
11 J.H.F. Jansen, C. Alderleistein, A J. van Bennekom, K van der Borg and A F.M. De Jong, Terrigenous supply of ^{10}Be and dating with ^{14}C and ^{10}Be in sediments of Angola Basin (SE Atlantic), Nucl Instr. Methods Phys. Res B29, 311–316, 1987.
12 R. Finkel, S. Krishnaswami and D L Clark, ^{10}Be in Arctic Ocean sediments, Earth Planet Sci Lett. 35, 199–204, 1977.
13 M.P. Bacon, D W. Spencer and P.G. Brewer, ^{210}Pb/^{226}Ra and ^{210}Po/^{210}Pb disequilibria in seawater and suspended particulate matter, Earth Planet. Sci. Lett. 32, 277–296, 1976
14 D.W. Spencer, M.P. Bacon and P.G Brewer, Models of the distribution of ^{210}Pb in a section across the North Equatorial Atlantic Ocean, J. Mar Res. 39, 119–138, 1981.
15 J.K. Cochran, M.P Bacon, S. Krishnaswami and K.K. Turekian, ^{210}Pb and ^{210}Po distributions in the central and eastern Indian Ocean, Earth Planet Sci Lett. 65, 433–452, 1983.
16 J.K. Cochran, T. McKibbin-Vaughan, M.M Dornblaser, D. Hirschberg, H.D. Livingston and K O. Buesseler, ^{210}Pb scavenging in the North Atlantic and North Pacific Oceans, Earth Planet. Sci Lett. 97, 332–352, 1990.
17 M. Koide and E.D. Goldberg, Transuranic nuclides in two coastal marine sediments off Peru, Earth Planet. Sci. Lett. 57, 263–277, 1982.
18 R.F Anderson, M.P. Bacon and P.G. Brewer, Removal of ^{230}Th and ^{231}Pa from the open ocean, Earth Planet. Sci. Lett. 62, 7–23, 1983a.
19 R F. Anderson, M P. Bacon and P.G. Brewer, Removal of ^{230}Th and ^{231}Pa at ocean margins, Earth Planet. Sci. Lett 66, 73–90, 1983b
20 H.-S. Yang, Y. Nozaki, Y. Sakai and A. Masuda, The distribution of ^{230}Th and ^{231}Pa in the deep surface sediments of the Pacific Ocean, Geochim Cosmochim. Acta 50, 81–89, 1986.
21 G B. Shimmield, J W. Murray, J. Thomson, M.P. Bacon, R.F. Anderson and N B. Price, The distribution and behavior of ^{230}Th and ^{231}Pa at an ocean margin, Baja California, Mexico, Geochim. Cosmochim. Acta 50, 2499–2507, 1986.
22 M P. Bacon, Tracers of chemical scavenging in the ocean: boundary effects and large-scale chemical fractionation, Philos. Trans. R. Soc London Ser. A 325, 147–160, 1988.
23 R.F Anderson, Y. Lao, W.S. Broecker, S.E. Trumbore, H.J Hofmann and W Wolfli, Boundary scavenging in the Pacific Ocean: a comparison of ^{10}Be and ^{231}Pa, Earth Planet. Sci Lett. 96, 287–304, 1990
24 Y. Lao, R.F. Anderson, W.S. Broecker, H.J. Hofmann and W. Wolfli, Particulate fluxes of ^{230}Th, ^{231}Pa and ^{10}Be in the Northeastern Pacific Ocean, Geochim. Cosmochim. Acta, 1992 (in press).
25 R.F. Anderson, M Q. Fleisher, P.E. Biscaye and N. Kumar, Anomalous boundary scavenging in the Middle Atlantic Bight: evidence from ^{230}Th, ^{231}Pa, ^{10}Be and ^{210}Pb, Continental Shelf Res., submitted.
26 Y. Lao, Transport and burial rates of ^{10}Be and ^{231}Pa in the Pacific Ocean, Ph.D. Thesis, Columbia Univ , 1991.
27 D.K Rea and M Leinen, Asian aridity and zonal westerlies. late Pleistocene and Holocene record of eolian deposition in the Northwest Pacific Ocean, Paleogeogr. Paleoclimatol , Paleoecol. 66, 1–8, 1988.
28 A M. Olivarez, R M. Owen and D.K Rea, Geochemistry of eolian dust in Pacific pelagic sediments implications for paleoclimatic interpretations, Geochim. Cosmochim. Acta 55, 2147–2158, 1991.
29 K. Bostrom, T. Kraemer and S. Gartner, Provenance and accumulation rates of opaline silica, Al, Ti, Fe, Mn, Cu, Ni, and Co in Pacific pelagic sediments, Chem Geol. 11, 123–148, 1973.
30 J. Kennett, Marine Geology, Prentice-Hall, Englewood Cliffs, N.J , 1982.
31 G.B. Shimmield and N.B. Price, The scavenging of U, ^{230}Th and ^{231}Pa during pulsed hydrothermal activity at 20°S, East Pacific Rise, Geochim. Cosmochim. Acta 52, 669–677, 1988
32 P. Sharma, R. Mahannah, W.S Moore, T.L. Ku and J.R. Southon, Transport of ^{10}Be and ^{9}Be in the ocean, Earth Planet Sci. Lett. 86, 69–76, 1987
33 D J DeMaster, The marine budgets of silica and ^{32}Si, Ph.D. Thesis, Yale Univ., 1979
34 K. Taguchi, K. Harada and S Tsunogai, Particulate removal of ^{230}Th and ^{231}Pa in the biologically productive northern North Pacific, Earth Planet. Sci Lett. 93, 223–232, 1989.
35 D L. Bourles, G. Klinkhammer, A C. Campbell, C.I. Measures, E.T. Brown and J.M. Edmond, Beryllium in marine pore waters: geochemical and geochronological implications, Nature 341, 731–733, 1989

36 C. Sancetta, L Heusser, L. Labeyrie, A.S. Naidu and S W. Robinson, Wisconsin–Holocene paleoenvironments of Bering Sea. evidence from diatoms, pollen, oxygen isotopes and clay minerals, Mar. Geol. 62, 55–68, 1985
37 A. Shemesh, R A. Mortlock and P.N. Froelich, Late Cenozoic Ge/Si record of marine biogenic opal· implication for variations of riverine fluxes to the ocean, Paleoceanography 4, 221–234, 1989.
38 P.N Froelich, R A. Mortlock and A. Shemesh, Inorganic germanium and silica in the Indian Ocean: biological fractionation during $(Ge/Si)_{OPAL}$ formation, Global Biogeochem Cycles 3, 79–88, 1989.
39 D. Kadko, A multitracer approach to the study of erosion in the northeast equatorial Pacific, Earth Planet. Sci Lett 63, 13–33, 1983
40 S.G McRae, Glauconite, Earth Sci. Rev. 8, 397–440, 1972
41 T. Vercoutere, H.T Mullens, K McDougall and J.B. Thompson, Sedimentation across the central California oxygen minimum zone· an alternative coastal upwelling sequence, J Sediment. Petrol 57, 709–722, 1987
42 M. Kusakabe, T.-L Ku, J R Southon, J S Vogel, D E Nelson, C I. Measures and Y. Nozaki, Distribution of ^{10}Be and ^{9}Be in the Pacific Ocean, Earth Planet Sci. Lett 82, 231–240, 1987.
43 H W. Menard and S.M Smith, Hypsometry of ocean basin provinces, J. Geophys Res. 71, 4305–4325, 1966.
44 S. Tanaka, T. Inoue and Z.Y. Huang, ^{10}Be and ^{10}Be/^{9}Be in near Antarctic sediment cores, Geochem. J. 16, 321–325, 1982.
45 M Lyle, R. Zahn, F. Prahl, J Dymond and R. Collier, Paleoproductivity and carbon burial across the California Current: the MULTITRACERS transect 42°N, Paleoceanography, 1992, in press
46 K Fisher, J Dymond and M. Lyle, The benthic cycle of copper evidence from sediment trap experiments in the eastern tropical North Pacific Ocean, Geochim Cosmochim Acta 50, 1535–1543, 1986
47 R. Chester, A Thomas, F J Lin, A.S Basaham and G Jacinto, The solid-state speciation of copper in surface water particulates and oceanic sediments, Mar. Chem. 24, 261–292, 1988.
48 J K B. Bishop, The barite–opal–organic carbon association in oceanic particulate matter, Nature 332, 341–343, 1988.
49 B Schmitz, Barium, equatorial high productivity and the northward wandering of the Indian continent, Paloceanography 2, 63–77, 1987
50 J Dymond, E. Suess and M. Lyle, Barium in deep-sea sediments. a geochemical proxy for paleoproductivity, Paleoceanography 7, 163–181, 1992
51 M P. Bacon and J N Rosholt, Accumulation of ^{230}Th, ^{231}Pa and some transition metals on the Bermuda Rise, Geochim Cosmochim. Acta 46, 651–666, 1982.
52 D.O. Suman and M.P Bacon, Variations in Holocene sedimentation in the North American Basin determined from Th-230 measurements, Deep-Sea Res 36, 869–878, 1989
53 M Kusakabe, T.-L. Ku, J R. Southon, S. Liu, J S Vogel, D.E. Nelson, S. Nakaya and G.L Cusinmano, Be isotopes in rivers/estuaries and their oceanic budgets, Earth Planet Sci Lett. 102, 265–276, 1991
54 T.L. Ku, M Kusakabe, C I Measures, J.R. Southon, J.S. Vogel, D E. Nelson and S. Nakaya, Be isotope distribution in the western North Atlantic· A comparison to the Pacific Deep-Sea Res 37, 795–808, 1990.
55 A.L. Gordon, Interocean exchange of thermocline water, J. Geophys Res. 90, 5037–5046, 1986
56 F. Terra, L Brown, J. Morris, I S. Sacks, J. Klein and R. Middleton, Sediment incorporation in island-arc magmas inference from ^{10}Be, Geochim. Cosmochim. Acta 50, 535–550, 1986.
57 J. Morris, W P Leeman and F Terra, The subducted component in island arc lavas constraints from Be isotopes and B–Be systematics, Nature 344, 31–36, 1990.
58 Y Lao, R F Anderson, W S. Broecker, S.E. Trumbore, H J. Hofmann and W Wolfli, Increased production of cosmogenic ^{10}Be during the Last Glacial Maximum, Nature 357, 576–578, 1992.